

Conservative, gravitational self-force for a particle in circular orbit around a Schwarzschild black hole in a Radiation Gauge

Abhay G. Shah,^{1,*} Tobias S. Keidl,^{2,†} John L. Friedman,^{1,‡} Dong-Hoon Kim,^{3,4,5,§} and Larry R. Price^{1,¶}

¹*Center for Gravitation and Cosmology, Department of Physics,
University of Wisconsin–Milwaukee, P.O. Box 413, Milwaukee, Wisconsin 53201, USA*

²*Department of Physics, University of Wisconsin–Washington County, USA*

³*Max-Planck-Institut für Gravitationsphysik, Am Mühlenberg 1, D-14476 Golm, Germany*

⁴*Division of Physics, Mathematics, and Astronomy,
California Institute of Technology, Pasadena, CA 91125, USA*

⁵*Institute for the Early Universe and Department of Physics,
Ewha Womans University, Seoul 120-750, South Korea*

(Dated: September 21, 2010)

This is the second of two companion papers on computing the self-force in a radiation gauge; more precisely, the method uses a radiation gauge for the radiative part of the metric perturbation, together with an arbitrarily chosen gauge for the parts of the perturbation associated with changes in black-hole mass and spin and with a shift in the center of mass. In a test of the method delineated in the first paper, we compute the conservative part of the self-force for a particle in circular orbit around a Schwarzschild black hole. The gauge vector relating our radiation gauge to a Lorenz gauge is helically symmetric, implying that the quantity $h_{\alpha\beta}u^\alpha u^\beta$ must have the same value for our radiation gauge as for a Lorenz gauge; and we confirm this numerically to one part in 10^{14} . As outlined in the first paper, the perturbed metric is constructed from a Hertz potential that is in turn obtained algebraically from the retarded perturbed spin-2 Weyl scalar, ψ_0^{ret} . We use a mode-sum renormalization and find the renormalization coefficients by matching a series in $L = \ell + 1/2$ to the large- L behavior of the expression for the self-force in terms of the retarded field $h_{\alpha\beta}^{\text{ret}}$; we similarly find the leading renormalization coefficients of $h_{\alpha\beta}u^\alpha u^\beta$ and the related change in the angular velocity of the particle due to its self-force. We show numerically that the singular part of the self-force has the form $f_\alpha^S = \langle \nabla_\alpha \rho^{-1} \rangle$, the part of $\nabla_\alpha \rho^{-1}$ that is axisymmetric about a radial line through the particle. This differs only by a constant from its form for a Lorenz gauge. It is because we do not use a radiation gauge to describe the change in black-hole mass that the singular part of the self-force has no singularity along a radial line through the particle and, at least in this example, is spherically symmetric to subleading order in ρ .

PACS numbers: 04.30.Db, 04.25.Nx, 04.70.Bw

I. INTRODUCTION

We present here a first self-force computation in a radiation gauge, following the method outlined in a companion paper [1] (henceforth Paper I). The computation has been done previously by Barack and Sago [2] and by Detweiler [3], and gauge invariant quantities associated with the conservative part of the self-force are compared in their joint paper [4]. A radiation-gauge approach has the advantage that one can use the Teukolsky equation to compute the perturbed metric and the self-force for orbits in a Kerr background, and the present paper serves as a test of methods described in Paper I for that problem.

The use of a radiation gauge for the self-force problem has been delayed in part because the MiSaTaQuWa renormalization prescription [5, 6] was developed for a Lorenz gauge and in part because, in a radiation gauge, the linearized metric of a point-particle is singular along a ray through the particle. One can avoid a singularity of this kind by restricting the use of a radiation gauge to the part of the perturbation determined by the gauge-invariant Weyl scalar ψ_0 (or ψ_4). The part of the metric perturbation that describes the change in mass and angular momentum of the spacetime can then be added in any convenient gauge. The perturbed metric obtained from from ψ_0 is constructed as

*Electronic address: agshah@uwm.edu

†Electronic address: tobias.keidl@uwc.edu

‡Electronic address: friedman@uwm.edu

§Electronic address: ki1313@yahoo.com

¶Electronic address: larry@gravity.phys.uwm.edu

a sum of angular and time harmonics, defined for $r > r_0$ and for $r < r_0$, with r_0 the Schwarzschild radial coordinate of the particle.

Although the $\ell \geq 2$ part of the metric perturbation can be computed more simply in a radiation gauge, an analytic computation of the singular field that is to be subtracted is significantly more difficult. We avoid the difficulty by replacing the analytic computation by a numerical determination of the renormalization coefficients that are subtracted in a mode-sum renormalization of the self-force. As a result, the efficacy of the method depends on the numerical accuracy with which these coefficients can be computed. We describe the numerical methods used and report tests of their accuracy.

As noted in Paper I, recent work by Gralla [7], following an earlier derivation of the self-force equations by Gralla and Wald [8], shows that the first order correction to the geodesic equation,

$$u^\beta \nabla_\beta u^\alpha = a^{\text{ren } \alpha}, \quad (1)$$

is obtained from

$$a^{\text{ret } \alpha} = -(g^{\alpha\delta} - u^\alpha u^\delta) \left(\nabla_\beta h_{\gamma\delta}^{\text{ret}} - \frac{1}{2} \nabla_\delta h_{\beta\gamma}^{\text{ret}} \right) u^\beta u^\gamma, \quad (2)$$

by an angle average in locally inertial coordinates, over a sphere of geodesic radius ρ about the particle:

$$a^{\text{ren } \mu} = \lim_{\rho \rightarrow 0} \int_{S_\rho} a^{\text{ret } \mu} d\Omega. \quad (3)$$

The equation holds in any gauge for which the leading part of $h_{\alpha\beta}^{\text{ren}}$ is $O(\rho^{-1})$ and has even parity. Paper I showed that the even-parity condition was satisfied in a radiation gauge. Taking the angle average is equivalent to subtracting a field a^s (the singular part of the acceleration)

$$a^{\text{ren } \alpha} = a^{\text{ret } \alpha} - a^{s \alpha}, \quad (4)$$

if $a^{s \alpha}$ satisfies the conditions (i) The limiting angle average of a^s , defined as in Eq. (3), vanishes; and (ii) $a^{\text{ret } \alpha} - a^{s \alpha}$ is continuous at the particle.

The numerical determination of $a^{s \alpha}$ from $a^{\text{ret } \alpha}$ shows, with an accuracy close to machine precision, that $a^{s \alpha}$ is proportional to $\langle \nabla^\alpha \rho^{-1} \rangle$ and hence is spherically symmetric. The result also implies that the singular field can be identified with its leading and subleading terms in its mode-sum expression as a power series in $L = \ell + 1/2$. It remains an open question whether this unexpectedly simple behavior of the singular part of a^α holds for generic orbits or for a Kerr background.

The plan of the paper is as follows. The perturbed metric is constructed from the Weyl scalar ψ_0^{ret} , computed as a sum over spin-weighted spherical harmonics, and Sec. II details the numerical method used to compute the retarded radial and angular functions that comprise the sum. In particular, radial integrations using the Teukolsky radial equation and the Sasaki-Nakamura form are used and compared. Sec. III describes the computation of the retarded metric and the retarded expression for the self force from the values of ψ_0 for each harmonic. The conservative part of the self force has only a radial component, f^r , and it is renormalized by matching a power series in L to the sequence of contributions $f^r[\ell]$ from successive angular harmonics. We find that the singular field obtained in this way is the angular decomposition of $\langle \nabla^\alpha \rho^{-1} \rangle$, with ρ the geodesic distance orthogonal to the particle's trajectory.

Associated with the perturbed metric of a particle in circular orbit is a set of related quantities that are invariant under helically symmetric gauge transformations. The Sago et al. comparison paper [4] tabulated values of one of these quantities, and we add the values from our radiation-gauge computation to their comparison table.

II. COMPUTATION OF ψ_0^{ret}

Formalism

We begin with a brief review of the formalism used in Paper I. We consider a particle of mass m in circular orbit about a Schwarzschild black hole of mass M . We use Schwarzschild coordinates, with the particle at radial coordinate r_0 in the $\theta = \pi/2$ -plane. The particle's four-velocity is

$$u^\alpha = u^t (t^\alpha + \Omega \phi^\alpha), \quad (5)$$

with t^α and ϕ^α timelike and rotational Killing vectors, $\Omega = \sqrt{M/r_0^3}$, and $u^t = 1/\sqrt{1 - 3M/r_0}$. With a δ -function is normalized by $\int \delta^4(x, z) \sqrt{|g|} d^4x = 1$, its stress-energy tensor is given by

$$\begin{aligned} T^{\alpha\beta} &= \mathbf{m} u^\alpha u^\beta \int \delta^4(x^a - z^a(\tau)) d\tau \\ &= \mathbf{m} \frac{u^\alpha u^\beta}{u^t (-g)^{1/2}} \delta(r - r_0) \delta(\cos \theta) \delta(\phi - \Omega t) \end{aligned} \quad (6)$$

where a change of coordinates from τ to t in the integral for stress-energy tensor is used to obtain the second equality. From the addition theorem for spin-weighted spherical harmonics, we have

$$T^{\alpha\beta} = \sum_{\ell, m} \frac{\mathbf{m} u^\alpha u^\beta}{r_0^2 u^t} \delta(r - r_0) {}_s Y_{\ell m}(\theta, \phi) {}_s \bar{Y}_{\ell m}(\pi/2, \Omega t). \quad (7)$$

The Kinnersley tetrad vectors have components

$$(l^\mu) = (1/f(r), 1, 0, 0), \quad (n^\mu) = \frac{1}{2}(1, -f(r), 0, 0), \quad (m^\mu) = \frac{1}{\sqrt{2}r}(0, 0, 1, i/\sin \theta), \quad (8)$$

where $f(r) := 1 - 2M/r$; and we denote by \mathbf{D} , $\mathbf{\Delta}$, and $\mathbf{\delta}$ the derivative operators along the tetrad vectors l , n and m , respectively. The nonvanishing spin-coefficients associated with this tetrad are

$$\varrho = -1/r, \quad \beta = -\alpha = \frac{\cot \theta}{2\sqrt{2}r}, \quad \mu = -\frac{\Delta}{2r^3}, \quad \text{and} \quad \gamma = \frac{M}{2r^2}, \quad (9)$$

where $\Delta = r^2 - 2Mr$.

The perturbed Weyl scalar $\psi_0 = -C_{\alpha\beta\gamma\delta} l^\alpha m^\beta l^\gamma m^\delta$ satisfies the Bardeen-Press equation (the Teukolsky equation for $a = 0$),

$$\left[\frac{r^4}{\Delta} \partial_t^2 - 4 \left(\frac{Mr^2}{\Delta} - r \right) \partial_t - \Delta^{-2} \frac{\partial}{\partial r} \left(\Delta^3 \frac{\partial}{\partial r} \right) - \bar{\delta} \delta \right] \psi_0 = 4\pi r^2 T, \quad (10)$$

where

$$\begin{aligned} T &:= -2(\mathbf{\delta} - 2\beta)\mathbf{\delta}T_{11} + 4(\mathbf{D} - 4\varrho)(\mathbf{\delta} - 2\beta)T_{13} - 2(\mathbf{D} - 5\varrho)(\mathbf{D} - \varrho)T_{33} \\ &= T^{(0)} + T^{(1)} + T^{(2)}. \end{aligned} \quad (11)$$

The superscripts indicate the maximum number of radial derivatives in each term. Explicitly,

$$T^{(0)} = - \sum_{\ell, m} \frac{\mathbf{m} u^t}{r_0^4} \delta(r - r_0) [(\ell - 1)\ell(\ell + 1)(\ell + 2)]^{1/2} {}_2 Y_{\ell m}(\theta, \phi) \bar{Y}_{\ell m} \left(\frac{\pi}{2}, \Omega t \right), \quad (12a)$$

$$T^{(1)} = \sum_{\ell, m} \frac{\mathbf{m} \Omega u^t}{r_0^2} \left[2i\delta'(r - r_0) + \frac{2m\Omega}{f_0} \delta(r - r_0) \right] [(\ell - 1)(\ell + 2)]^{1/2} {}_2 Y_{\ell m}(\theta, \phi) {}_1 \bar{Y}_{\ell m} \left(\frac{\pi}{2}, \Omega t \right), \quad (12b)$$

$$\begin{aligned} T^{(2)} &= \sum_{\ell m} \mathbf{m} \Omega^2 u^t \left[\delta''(r - r_0) + \left(\frac{6}{r_0} - \frac{2im\Omega}{f_0} \right) \delta'(r - r_0) \right. \\ &\quad \left. - \left(\frac{m^2 \Omega^2}{f_0^2} + \frac{6im\Omega}{r_0 f_0} + \frac{2imM\Omega}{r_0^2 f_0^2} \right) \delta(r - r_0) \right] {}_2 Y_{\ell m}(\theta, \phi) {}_2 \bar{Y}_{\ell m} \left(\frac{\pi}{2}, \Omega t \right). \end{aligned} \quad (12c)$$

The Weyl scalar has the harmonic decomposition

$$\psi_0 = \sum_{\ell m} e^{-i\omega_m t} R_{0\ell\omega_m}(r) {}_2 Y_{\ell m}(\theta, \phi), \quad \omega_m := m\Omega. \quad (13)$$

Its radial functions $R_{0\ell\omega_m}$ and the corresponding radial functions $R_{4\ell\omega_m}$ of $\varrho^{-4}\psi_4$ satisfy (ℓ and ω_m subscripts suppressed)

$$\Delta R_0'' + 6(r - M)R_0' + \left[\frac{\omega^2 r^4}{\Delta} + \frac{4i\omega r^2(r - 3M)}{\Delta} - (\ell - 2)(\ell + 3) \right] R_0 = 0, \quad (14)$$

$$\Delta R_4'' - 2(r - M)R_4' + \left[\frac{\omega^2 r^4}{\Delta} - \frac{4i\omega r^2(r - 3M)}{\Delta} - (\ell - 1)(\ell + 2) \right] R_4 = 0, \quad (15)$$

where the prime denotes a derivative with respect to the radial coordinate r . Solutions to the above equations are related by

$$R_0 = \frac{\bar{R}_4}{r^4 f^2}; \quad (16)$$

in this relation, however, R_0 and R_4 differ by a relative normalization from the radial functions of components ψ_0 and ψ_4 of the same vacuum Weyl tensor.

We denote by R_{H} and R_{∞} solutions to Eq. (14) that are regular at the horizon and at infinity, respectively, and will write $(') := \frac{d}{dr}$. As shown in Sect. V of paper I, the solution to Eq. (10) is given by

$$\psi_0 = \psi_0^{(0)} + \psi_0^{(1)} + \psi_0^{(2)}, \quad (17)$$

where the three terms, corresponding to the three source terms of Eq. (12), have the form

$$\psi_0^{(0)} = 4\pi m u^t \frac{\Delta_0^2}{r_0^2} \sum_{\ell m} A_{\ell m} [(\ell-1)\ell(\ell+1)(\ell+2)]^{1/2} R_{\text{H}}(r_{<}) R_{\infty}(r_{>}) {}_2Y_{\ell m}(\theta, \phi) \bar{Y}_{\ell m}\left(\frac{\pi}{2}, \Omega t\right), \quad (18a)$$

$$\begin{aligned} \psi_0^{(1)} = 8\pi i m \Omega u^t \Delta_0 \sum_{\ell m} A_{\ell m} [(\ell-1)(\ell+2)]^{1/2} {}_2Y_{\ell m}(\theta, \phi) {}_1\bar{Y}_{\ell m}\left(\frac{\pi}{2}, \Omega t\right) \times \\ \left\{ [im\Omega r_0^2 + 2r_0] R_{\text{H}}(r_{<}) R_{\infty}(r_{>}) + \Delta_0 [R'_{\text{H}}(r_0) R_{\infty}(r) \theta(r-r_0) + R_{\text{H}}(r) R'_{\infty}(r_0) \theta(r_0-r)] \right\}, \end{aligned} \quad (18b)$$

$$\begin{aligned} \psi_0^{(2)} = -4\pi m \Omega^2 u^t \sum_{\ell m} A_{\ell m} {}_2Y_{\ell m}(\theta, \phi) {}_2\bar{Y}_{\ell m}\left(\frac{\pi}{2}, \Omega t\right) \times \\ \left\{ [30r_0^4 - 80Mr_0^3 + 48M^2r_0^2 - m^2\Omega^2r_0^6 - 2\Delta_0^2 - 24\Delta_0r_0(r_0-M) + 6im\Omega r_0^4(r_0-M)] R_{\text{H}}(r_{<}) R_{\infty}(r_{>}) \right. \\ + 2(6r_0^5 - 20Mr_0^4 + 16M^2r_0^3 - 3r_0\Delta_0^2 + im\Omega\Delta_0r_0^4) [R'_{\text{H}}(r_0) R_{\infty}(r) \theta(r-r_0) + R'_{\infty}(r_0) R_{\text{H}}(r) \theta(r_0-r)] \\ \left. + r_0^2 \Delta_0^2 [R''_{\text{H}}(r_0) R_{\infty}(r) \theta(r-r_0) + R''_{\infty}(r_0) R_{\text{H}}(r) \theta(r_0-r) + W[R_{\text{H}}(r), R_{\infty}(r)] \delta(r-r_0)] \right\}. \end{aligned} \quad (18c)$$

Here the Wronskian-related quantity,

$$A_{\ell m} := \frac{1}{\Delta^3 (R_{\text{H}} R'_{\infty} - R_{\infty} R'_{\text{H}})}, \quad (19)$$

is a constant, independent of r .

Numerical method

To compute ψ_0^{ret} , we use a 7th order Runge-Kutta routine to integrate the radial Teukolsky equation, matching the radial function to a power series expansion near the horizon and infinity. Because our renormalization method relies on numerical extraction of the renormalization coefficients, we work to high numerical precision and check the results by comparing independent codes based on the Teukolsky form of the radial equation (14) and on the Sasaki-Nakamura form. We find the spin-weighted spherical harmonics ${}_sY_{\ell m}(\frac{\pi}{2}, 0)$ to similarly high precision.

Because one of solutions for R_0 diverges at the horizon, we integrate R_4 from the horizon and R_0 from infinity. We match near the horizon and at large r , respectively, to the series expansions

$$R_4^{\text{H}} = e^{i\omega r^*} \sum_n a_n \left(\frac{r}{M} - 2\right)^n, \quad (20)$$

$$R_{0\infty} = e^{i\omega r^*} \sum_n \frac{b_n}{(r/M)^{n+5}}, \quad (21)$$

where $r^* = r + 2M \log(r/2M - 1)$. The expansion coefficients are found from a 3-term recurrence relation,

$$a_n = \frac{-2i\omega M(n-5)a_{n-2} + (\ell^2 + \ell - 6 + 5n - n^2 - 8i\omega M + 20i\omega M)a_{n-1}}{2n(n-2 + 4i\omega M)}, \quad (22)$$

$$b_n = \frac{i}{2n\omega M} ((6 + 8n + 2n^2)b_{n-2} + (\ell^2 + \ell - 2 - 3n - n^2)b_{n-1}), \quad (23)$$

obtained by substitution in Eqs. (14) and (15). The integrations from the horizon and from infinity yield the two independent solutions to the homogenous Teukolsky equation that we have labeled R_H and R_∞ . By using the outgoing wave solution at the event horizon as an initial condition for R_4^H , we get the correct boundary condition (ingoing at horizon) for $s = +2$ radial solution on using Eq. (16) i.e.

$$R_0^H \sim \frac{e^{-i\omega r^*}}{r^4 f^2}. \quad (24)$$

The numeric results are compared with the numerical solution obtained from Sasaki-Nakamura equation for consistency. In this case, we integrate

$$\frac{d^2 X_{\ell,m,\omega}}{dr^{*2}} = U(r) X_{\ell,m,\omega}, \quad (25)$$

where

$$U(r) = \frac{12M^2 - 2Mr(\ell^2 + \ell + 3) + r^2(\ell^2 + \ell - r^2\omega^2)}{r^4}. \quad (26)$$

The function $X_{\ell,m,\omega}$ is related to the homogenous solution of the $s = -2$ radial, Teukolsky equation by

$${}_4R_{\ell,m,\omega} = \frac{2\Delta(r - 3M + ir^2\omega)}{\eta r} X'_{\ell,m,\omega} + \left(\frac{l(l+1)\Delta}{\eta r} - \frac{6M\Delta}{\eta r^2} - \frac{2r\omega(3iM - ir + r^2\omega)}{\eta} \right) X_{\ell,m,\omega}, \quad (27)$$

where $\eta = (l-1)l(l+1)(l+2) - 12iM\omega$. We use a 7th order Runge-Kutta routine to integrate Eq.(25) with the boundary conditions

$$X_{\ell,m,\omega}^H = e^{i\omega r^*} \sum_n c_n \left(\frac{r}{M} - 2 \right)^n, \quad (28)$$

$$X_{\ell,m,\omega}^\infty = e^{-i\omega r^*} \sum_n \frac{d_n}{(r/M)^n}, \quad (29)$$

where $c_n = d_n = 0$ for $n < 0$. The values of c_n and d_n are calculated from the following recurrence relations:

$$c_n = -\frac{i(n-3)M\omega}{2n(n+4iM\omega)} c_{n-3} + \frac{\ell^2 + \ell - (n-2)(n-3 + 12iM\omega)}{4n(n+4iM\omega)} c_{n-2}, \quad (30)$$

$$+ \frac{\ell^2 + \ell - 2n^2 + 5n - 6 - 12i(n-1)M\omega}{2n(n+4iM\omega)} c_{n-1},$$

$$d_n = -i \frac{(n-3)(n+1)}{2nM\omega} d_{n-2} - i \frac{(\ell+n)(\ell-n+1)}{2nM\omega} d_{n-1}. \quad (31)$$

The outgoing (ingoing) boundary condition at infinity (event horizon) is used in combination with Eq. (16) which relates the $s = 2$ and $s = -2$ radial solutions.

The accuracy of the homogenous solutions is monitored by the constancy of $A_{\ell m}^{-1} = \Delta^3 W(R_H, R_\infty)$. Table I shows the fractional standard deviation (f.s.d.), or the departure of $\Delta^3 W$ from its average value. A comparison of the $s = \pm 2$ radial functions given by the Teukolsky equation and the Sasaki-Nakamura equation (Eqs. (14) and (15)) are included. Measured in this way, direct integration of the Teukolsky form yields 13-digit accuracy. Table II reports a second check of numerical accuracy by directly comparing the radial functions computed from the two forms of the radial equation.

ℓ	$M\omega$	f.s.d.(T-eqn)	f.s.d.(SN-eqn)
3	0.001	4.2×10^{-14}	2.8×10^{-14}
2	0.136083	2.8×10^{-14}	9.7×10^{-13}
5	0.000353553	4.4×10^{-14}	2.7×10^{-14}
5	0.340207	3.5×10^{-14}	1.3×10^{-12}
10	0.00108866	5.6×10^{-14}	4.3×10^{-14}
9	0.612372	4.3×10^{-14}	1.0×10^{-12}
14	0.000715542	6.2×10^{-14}	5.5×10^{-14}
15	1.02062	5.1×10^{-14}	1.1×10^{-12}
20	0.000929429	7.8×10^{-14}	7.4×10^{-14}
21	1.42887	5.9×10^{-14}	1.4×10^{-12}
25	0.000707107	9.2×10^{-14}	9.7×10^{-14}
25	1.70103	7.2×10^{-14}	1.1×10^{-12}
30	0.002	1.0×10^{-13}	1.2×10^{-13}
31	2.10928	8.0×10^{-14}	1.6×10^{-12}
35	0.000544331	1.2×10^{-13}	1.2×10^{-13}
34	2.31341	8.9×10^{-14}	1.1×10^{-12}
40	0.000988212	1.3×10^{-13}	1.5×10^{-13}
40	2.72166	9.6×10^{-14}	1.6×10^{-12}
45	0.000603682	1.5×10^{-13}	1.7×10^{-13}
46	3.1299	1.1×10^{-13}	1.3×10^{-12}
50	0.000353553	1.6×10^{-13}	1.8×10^{-13}
50	3.40207	1.2×10^{-13}	1.5×10^{-12}
55	0.00067466	1.8×10^{-13}	2.0×10^{-13}
55	3.74228	1.3×10^{-13}	1.1×10^{-12}
60	0.001	2.0×10^{-13}	2.3×10^{-13}
61	4.15052	1.3×10^{-13}	1.5×10^{-12}
65	0.000544331	2.2×10^{-13}	2.5×10^{-13}
64	4.35465	1.4×10^{-13}	1.5×10^{-12}
71	0.000494106	2.3×10^{-13}	2.8×10^{-13}
70	4.7629	1.7×10^{-13}	1.4×10^{-12}
75	0.000637528	2.5×10^{-13}	3.1×10^{-13}
74	5.03506	1.8×10^{-13}	1.5×10^{-12}
80	0.000471818	2.8×10^{-13}	3.5×10^{-13}
80	5.44331	1.9×10^{-13}	1.5×10^{-12}
85	0.000707107	3.0×10^{-13}	3.9×10^{-13}
85	5.78352	2.1×10^{-13}	1.0×10^{-12}

TABLE I: Accuracy of radial integration measured by fractional standard deviation (f.s.d) of $\Delta^3 W$ from its average value, for specified ℓ and ω . The third and fourth columns list the f.s.d. obtained by integrating the Teukolsky and Sasaki-Nakamura forms of the radial equation, respectively. The frequencies are chosen to lie between the maximum and minimum of $m\Omega$, between the value $M\omega = \ell/6^{3/2}$ at the ISCO and $M\omega \sim 1/150^{3/2}$, at $r_0 \sim 150M$, $m = 1$. The f.s.d. in the region $r = 6M$ to $20M$ is usually twice the average shown above.

To calculate ${}_s Y_{\ell m}$ to high precision, we used the following analytical forms of spin-weighted harmonics at $\theta = \pi/2$.

r_0/M	ℓ	m	fractional difference
100	2	1	5.9×10^{-13}
10	2	2	4.6×10^{-15}
6	2	1	1.9×10^{-13}
80	75	75	1.7×10^{-15}
80	20	1	3.2×10^{-15}
13	5	4	1.6×10^{-14}
10	3	1	2.3×10^{-14}
8	15	14	5.0×10^{-15}
8	12	6	1.6×10^{-14}
70	3	2	1.8×10^{-15}
6	4	1	4.1×10^{-13}
50	4	1	1.0×10^{-13}
6	10	9	4.7×10^{-13}
70	9	8	1.7×10^{-15}
6	25	1	4.0×10^{-16}
7	25	25	2.4×10^{-15}
75	19	18	5.0×10^{-15}
6	20	20	2.0×10^{-14}
72	85	78	1.5×10^{-15}
6	85	85	2.4×10^{-14}
7	85	5	4.2×10^{-14}
60	75	1	4.0×10^{-16}
10	75	71	2.2×10^{-15}
15	50	38	1.4×10^{-15}
6	40	25	7.2×10^{-15}
6	25	15	7.1×10^{-15}
30	25	1	6.0×10^{-16}
20	25	25	7.8×10^{-15}
10	2	1	3.9×10^{-14}

TABLE II: For each listed value of ℓ , m and r_0 , we give the fractional difference between the radial functions at r_0 , obtained by integrating the Teukolsky and the Sasaki-Nakamura forms of the radial equation, with frequency $\omega = m\Omega = mM^{1/2}r_0^{-3/2}$.

Introducing the symbol $e_{\ell,m} := \begin{cases} 1 & \ell + m \text{ even} \\ 0, & \ell + m \text{ odd} \end{cases}$, we can write

$$Y_{\ell m}\left(\frac{\pi}{2}, 0\right) = (-1)^{(\ell+m)/2} \frac{\sqrt{(2\ell+1)(\ell-m)!(\ell+m)!}}{\sqrt{4\pi}(\ell-m)!(\ell+m)!} e_{\ell,m}, \quad (32)$$

$${}_1Y_{\ell m}\left(\frac{\pi}{2}, 0\right) = (-1)^{(\ell+m)/2} \sqrt{\frac{(2\ell+1)(\ell-m)!(\ell+m)!}{4\pi\ell(\ell+1)}} \left[\frac{m e_{\ell,m}}{(\ell-m)!(\ell+m)!} - \frac{i e_{\ell,m+1}}{(\ell-m-1)!(\ell+m-1)!} \right], \quad (33)$$

$${}_2Y_{\ell m}\left(\frac{\pi}{2}, 0\right) = (-1)^{(\ell+m)/2} \sqrt{\frac{(2\ell+1)(\ell-m)!(\ell+m)!}{4\pi(\ell-1)\ell(\ell+1)(\ell+2)}} \left[\frac{[2m^2 - \ell(\ell+1)] e_{\ell,m}}{(\ell-m)!(\ell+m)!} - \frac{2i m e_{\ell,m+1}}{(\ell-m-1)!(\ell+m-1)!} \right]. \quad (34)$$

In this way, we obtain values of ψ_0^{ret} with accuracy of 1 part in 10^{13} .

III. METRIC PERTUBATION AND SELF-FORCE

We use the outgoing radiation gauge (ORG) satisfying the conditions

$$h_{\alpha\beta}n^\alpha = 0, \quad h = 0. \quad (35)$$

We find the retarded perturbed metric from a Hertz potential Ψ^{ret} satisfying

$$8\psi_0^{\text{ret}} = \bar{\partial}^4 \bar{\Psi}^{\text{ret}} + 12M\partial_t \Psi^{\text{ret}}, \quad (36)$$

whose algebraic solution for each angular harmonic is given by

$$\Psi_{\ell m} = 8 \frac{(-1)^m (\ell+2)(\ell+1)\ell(\ell-1)\bar{\psi}_{\ell,-m} + 12imM\Omega\psi_{\ell m}}{[(\ell+2)(\ell+1)\ell(\ell-1)]^2 + 144m^2M^2\Omega^2} \quad (37)$$

where $\Psi = \sum_{\ell,m} \Psi_{\ell m}(r) {}_2Y_{\ell m}(\theta, \phi)e^{-im\Omega t}$ and $\psi_0 = \sum_{\ell,m} \psi_{\ell m}(r) {}_2Y_{\ell m}(\theta, \phi)e^{-im\Omega t}$.

The ORG form of the metric perturbation $h_{\alpha\beta}$ is

$$h_{\alpha\beta} = r^4 \{ n_\alpha n_\beta (\bar{\delta} + 2\beta)(\bar{\delta} + 4\beta) + \bar{m}_\alpha \bar{m}_\beta (\Delta + 5\mu - 2\gamma)(\Delta + \mu - 4\gamma) - n_{(\alpha} \bar{m}_{\beta)} [(\bar{\delta} + 4\beta)(\Delta + \mu - 4\gamma) + (\Delta + 4\mu - 4\gamma)(\bar{\delta} + 4\beta)] \} \Psi + \text{c.c.}, \quad (38)$$

where the spin coefficients are given by Eq. (9). After writing δ in terms of $\bar{\delta}$, the tetrad components take the form

$$h_{11} = \frac{r^2}{2} (\bar{\delta}^2 \Psi + \bar{\partial}^2 \bar{\Psi}), \quad (39)$$

$$h_{33} = r^4 \left[\frac{\partial_t^2 - 2f\partial_t\partial_r + f^2\partial_r^2}{4} - \frac{3(r-M)}{2r^2} \partial_t + \frac{f(3r-2M)}{2r^2} \partial_r + \frac{r^2 - 2M^2}{r^4} \right] \Psi, \quad (40)$$

$$h_{13} = -\frac{r^3}{2\sqrt{2}} \left(\partial_t - f\partial_r - \frac{2}{r} \right) \bar{\delta} \Psi. \quad (41)$$

Finally, the self-acceleration,

$$a^\alpha = -(g^{\alpha\delta} - u^\alpha u^\delta) \left(\nabla_\beta h_{\gamma\delta}^{\text{ren}} - \frac{1}{2} \nabla_\delta h_{\beta\gamma}^{\text{ren}} \right) u^\beta u^\gamma, \quad (42)$$

written in terms of these tetrad components, is given by

$$a^r = (u^t)^2 \left\{ f_0^2 \left[\frac{1}{16} f_0 \mathbf{D} + \frac{3}{8} \Delta + \frac{i}{8} \Omega (\bar{\delta} - \bar{\delta}) - \frac{1}{2} \frac{M}{r_0^2} \right] h_{11} + f_0 \left[\left(\frac{1}{8} \frac{M}{r_0} \mathbf{D} - \frac{1}{4} \frac{M}{r_0} \Delta + \frac{1}{2} \frac{M}{r_0^2} \right) h_{33} + \left(-\frac{i}{\sqrt{2}} \Omega r_0 \Delta + \frac{1}{4\sqrt{2}} \frac{M}{r_0^2} (\bar{\delta} - \bar{\delta}) + \frac{i}{2\sqrt{2}} \Omega \right) h_{13} + \text{c.c.} \right] \right\} \quad (43)$$

The harmonic decomposition, $\Psi = \sum_{\ell m} \Psi_{\ell m}(r) {}_2Y_{\ell m}(\theta, \phi)e^{-im\Omega t}$, of the Hertz potential gives a corresponding decomposition of a^r . The contribution to a^r from the harmonic $\Psi_{\ell m}$, however, is not a single angular harmonic because the particle's velocity u^α involves the Killing vector ϕ^α , an axial $\ell = 1$ vector field on the 2-sphere; and u^α occurs quadratically in Eq. (42) for a^r . Instead, the terms in Eq. (43) include terms from h_{11} and $\bar{\delta}h_{13}$ proportional to $Y_{\ell m}$; terms from $\bar{\delta}h_{11}$ and h_{13} proportional to ${}_1Y_{\ell m}$; and terms from $\bar{\delta}h_{13}$ and h_{33} proportional to ${}_2Y_{\ell m}$. A virtue of our numerical renormalization procedure is that we need not rewrite these latter terms as sums of spin-weight zero harmonics.

We organize the computation by writing the right side of Eq. (43) as a sum of six terms for which the magnitude $|s|$ of the spin-weight increases from one red square bracket to the next:

$$a^r = \left[(u^t)^2 f_0^2 \left(\frac{1}{16} f_0 \mathbf{D} + \frac{3}{8} \Delta - \frac{1}{2} \frac{M}{r_0^2} \right) h_{11} - \frac{1}{4\sqrt{2}} (u^t)^2 \frac{M f_0}{r_0^2} (\bar{\delta} h_{13} + \bar{\delta} h_{14}) \right] + \left[\frac{i}{8} (u^t)^2 f_0^2 \Omega (\bar{\delta} - \bar{\delta}) h_{11} - \frac{i}{\sqrt{2}} (u^t)^2 \Omega f_0 (r_0 \Delta - \frac{1}{2}) (h_{13} - h_{14}) \right] + \left[\frac{1}{4\sqrt{2}} (u^t)^2 \frac{f_0 M}{r_0^2} (\bar{\delta} h_{13} + \bar{\delta} h_{14}) + (u^t)^2 \frac{M f_0}{r_0} \left(\frac{1}{8} \mathbf{D} - \frac{1}{4f_0} \Delta + \frac{1}{2r_0} \right) (h_{33} + h_{44}) \right] \quad (44)$$

$$= \sum_{i=1}^6 a_i^r. \quad (45)$$

The subscript i ($i = 1, \dots, 6$) in the symbol a_i^r refers to the location of the term on the right side of Eq (44). We denote by $a^r[\ell]$ the contribution to a^r from the restriction of Ψ to the ℓ -subspace, writing

$$a^r[\ell] = \sum_{i=1}^6 a_i^r[\ell]. \quad (46)$$

The harmonics $a_i^r[\ell]$ have finite limits as $r \rightarrow r_0^\pm$. We evaluate a^r at a particle position P with coordinates $t = 0$, $\theta = \pi/2$, and $\phi = 0$, where the value of ${}_s Y_{\ell m}$ is real. The harmonics then have at P (for either choice of limit) the forms

$$a_1^r[\ell] = -\frac{1}{8}[(\ell-1)\ell(\ell+1)(\ell+2)]^{1/2}(u^t)^2 f_0^2 r_0^2 \left[-2\partial_t + f_0 \left(\partial_r + \frac{2}{r} \right) + 4\frac{M}{r_0^2} \right] \sum_m \text{Re}(\Psi_{\ell m}) Y_{\ell m}, \quad (47a)$$

$$a_2^r[\ell] = \frac{1}{8}[(\ell-1)\ell(\ell+1)(\ell+2)]^{1/2}(u^t)^2 M r_0 f_0 \sum_m \left[m\Omega \text{Im}(\Psi_{\ell m}) - \left(f_0 \partial_r + \frac{2}{r_0} \right) \text{Re}(\Psi_{\ell m}) \right] Y_{\ell m}, \quad (47b)$$

$$a_3^r[\ell] = -\frac{1}{8}\ell(\ell+1)[(\ell-1)(\ell+2)]^{1/2}(u^t)^2 f_0^2 r_0^2 \Omega \sum_m \text{Im}(\Psi_{\ell m}) ({}_1 Y_{\ell m} + {}_{-1} Y_{\ell m}), \quad (47c)$$

$$a_4^r[\ell] = \frac{1}{4}[(\ell-1)(\ell+2)]^{1/2}(u^t)^2 f_0 r_0^4 \Omega \left(\partial_t^2 - 2f_0 \partial_t \partial_r + f_0^2 \partial_r^2 - \frac{3}{r_0}(1+f_0)\partial_t + \frac{2f_0}{r_0} \left(3 - 2\frac{M}{r_0} \right) \partial_r + \frac{2}{r_0^2}(1+2f_0) \right) \sum_m \text{Im} \Psi_{\ell m} {}_1 Y_{\ell m}, \quad (47d)$$

$$a_5^r[\ell] = \frac{1}{8}(\ell-1)(\ell+2)(u^t)^2 f_0 M r_0 \sum_m (m\Omega \text{Im}(\Psi_{\ell m}) - f_0 \partial_r \text{Re}(\Psi_{\ell m}) - 2/r \text{Re}(\Psi_{\ell m})) {}_2 Y_{\ell m}, \quad (47e)$$

$$a_6^r[\ell] = \frac{1}{8}(u^t)^2 f_0 M r_0^3 \left[\partial_t^2 \partial_r - 2f_0 \partial_t \partial_r^2 + f_0^2 \partial_r^3 + \frac{6}{r_0} \partial_t^2 - 2(9 - 13M/r_0) \partial_t \partial_r + 12\frac{f_0}{r_0}(1 - M/r_0) \partial_r^2 - \frac{6}{r_0^2}(5 - 4M/r_0) \partial_t + \frac{2}{r_0^2}(17 - 32M/r_0 + 8M^2/r_0^2) \partial_r + \frac{16}{r_0^3}(1 - M^2/r_0^2) \right] \sum_m \text{Re}(\Psi_{\ell m}) {}_2 Y_{\ell m}. \quad (47f)$$

The mode-sum renormalization of the self-acceleration is given by

$$a^{\text{ren } r} = \lim_{\ell_{\text{max}} \rightarrow \infty} \sum_{\ell=0}^{\ell_{\text{max}}} (a^{\text{ret } r}[\ell] - a^{\text{s } r}[\ell]), \quad (48)$$

with $a^{\text{s } r}[\ell]$ the singular part of $a^{\text{ret } r}[\ell]$. As described in paper I, one can identify $a^{\text{s } r}[\ell]$ with the leading and subleading terms in L in the large- L expansion of $a^{\text{ret } r}$. This expansion has the (direction-dependent) form

$$a^{\text{ret } r}[\ell] = A^\pm \left(\ell + \frac{1}{2} \right) + B + \sum_{k=1}^{\infty} \frac{\tilde{E}_{2k}}{L^{2k}} + \tilde{a}_\ell^{\text{ren } r}, \quad (49)$$

where \tilde{a}_ℓ falls off at large ℓ faster than any power of ℓ , and the superscript \pm refers to the limit $r \rightarrow r_0^\pm$. Because we find that the singular field can be identified with its leading and subleading terms, the remaining part of the power-series expansion in L must sum to zero, and we reorder the higher-order terms in the power series, replacing L^k by a sequence of polynomials $P_{2k}(\ell)$ that individually sum to zero and whose leading term is L^k (see Eq. (74), below). We find the singular field numerically by matching a power-series of this form, truncated at a finite value k_{max} of k , to the sequence $a^{\text{ret } r}[\ell]$, computed using Eqs. (46) and (47). Since the ℓ -mode expansion of the singular field agrees with the large- ℓ expansion of the retarded field, one can extract the regularization parameters by the above method. Though we find the singular field ψ_0^{s} to order $O(\epsilon^{-1})$ in the previous paper, one can see that it takes a heavy amount of analytic work to calculate each of the $a_i^{\text{s } r}[\ell]$ which requires a careful analysis of more than 200 terms! Hence, we employ this numerical matching method to extract the renormalization coefficients in the radiation gauge.

A striking feature of the numerically determined singular field is that the first three terms in the L expansion of the conservative part f^r of the self-force coincide with the expression for $a^{\text{s } r}$ obtained from the power-series expansion of $\langle \nabla^r \rho^{-1} \rangle$. That is, the average over Φ of $\partial^r \frac{1}{\rho}$ is given by

$$\langle \partial^r \rho^{-1} \rangle = \sum_\ell [A^\pm L + B] + O(\rho), \quad (50)$$

r_0/M	A^+	B	red $\frac{A^+}{A^+_{\text{analytic}}}$ - 1	$\left \frac{B}{B_{\text{analytic}}} \right - 1$
6	$-1.964185503296099 \times 10^{-2}$	$-9.719920769918032 \times 10^{-3}$	6.8×10^{-14}	-5.0×10^{-11}
7	$-1.542712134731597 \times 10^{-2}$	$-7.595781032643107 \times 10^{-3}$	3.7×10^{-14}	-3.0×10^{-11}
8	$-1.235264711003273 \times 10^{-2}$	$-6.072295959309139 \times 10^{-3}$	$< 10^{-16}$	-5.7×10^{-12}
9	$-1.008020470281125 \times 10^{-2}$	$-4.954081856693618 \times 10^{-3}$	1.8×10^{-14}	-3.3×10^{-12}
10	$-8.366600265340854 \times 10^{-3}$	$-4.113353788131433 \times 10^{-3}$	1.2×10^{-14}	-7.3×10^{-12}
11	$-7.047957565474786 \times 10^{-3}$	$-3.467126055149815 \times 10^{-3}$	8.9×10^{-15}	-3.7×10^{-12}
12	$-6.014065304058753 \times 10^{-3}$	$-2.960554843842139 \times 10^{-3}$	2.5×10^{-14}	-1.1×10^{-11}
13	$-5.189692421934956 \times 10^{-3}$	$-2.556541533529994 \times 10^{-3}$	-2.4×10^{-14}	6.5×10^{-12}
14	$-4.522475818510165 \times 10^{-3}$	$-2.229391187912286 \times 10^{-3}$	8.4×10^{-14}	-2.9×10^{-11}
15	$-3.975231959999661 \times 10^{-3}$	$-1.960906506358998 \times 10^{-3}$	8.9×10^{-15}	-3.6×10^{-12}
16	$-3.521046167445508 \times 10^{-3}$	$-1.737934146698723 \times 10^{-3}$	5.8×10^{-14}	-1.7×10^{-11}
17	$-3.140087242121197 \times 10^{-3}$	$-1.550788700414580 \times 10^{-3}$	-4.6×10^{-15}	-6.7×10^{-15}
18	$-2.817502867825028 \times 10^{-3}$	$-1.392217662603554 \times 10^{-3}$	3.5×10^{-14}	-1.1×10^{-11}
19	$-2.542002591363557 \times 10^{-3}$	$-1.256707170227638 \times 10^{-3}$	-3.1×10^{-15}	9.4×10^{-13}
20	$-2.304886114323209 \times 10^{-3}$	$-1.140007036978271 \times 10^{-3}$	-5.7×10^{-15}	1.8×10^{-12}
25	$-1.500933043143495 \times 10^{-3}$	$-7.437542878990537 \times 10^{-4}$	-1.6×10^{-15}	-3.0×10^{-14}
30	$-1.054092553389464 \times 10^{-3}$	$-5.230319186714355 \times 10^{-4}$	4.2×10^{-15}	-1.1×10^{-12}
35	$-7.805574591571754 \times 10^{-4}$	$-3.876932093890911 \times 10^{-4}$	2.6×10^{-14}	-6.5×10^{-12}
40	$-6.011057519272318 \times 10^{-4}$	$-2.987922074634742 \times 10^{-4}$	3.8×10^{-15}	-8.5×10^{-13}
45	$-4.770823620144716 \times 10^{-4}$	$-2.372891353438443 \times 10^{-4}$	9.3×10^{-15}	-2.5×10^{-12}
50	$-3.878143885933070 \times 10^{-4}$	$-1.929854912525034 \times 10^{-4}$	1.8×10^{-15}	-2.3×10^{-13}
55	$-3.214363205318354 \times 10^{-4}$	$-1.600201924066196 \times 10^{-4}$	6.9×10^{-15}	-1.7×10^{-12}
60	$-2.707442873558057 \times 10^{-4}$	$-1.348310298624353 \times 10^{-4}$	4.2×10^{-15}	-9.6×10^{-13}
65	$-2.311598761671936 \times 10^{-4}$	$-1.151520162987173 \times 10^{-4}$	2.0×10^{-16}	-8.0×10^{-14}
70	$-1.996605675599292 \times 10^{-4}$	$-9.948607781191319 \times 10^{-5}$	-2.0×10^{-16}	-5.0×10^{-14}
75	$-1.741859372645818 \times 10^{-4}$	$-8.681200066822863 \times 10^{-5}$	1.3×10^{-15}	-3.4×10^{-13}
80	$-1.532923192995987 \times 10^{-4}$	$-7.641384666121239 \times 10^{-5}$	2.7×10^{-15}	-5.6×10^{-13}
85	$-1.359438646187131 \times 10^{-4}$	$-6.777766234583098 \times 10^{-5}$	-3.0×10^{-16}	2.9×10^{-13}

TABLE III: The first column shows the radius of the orbiting particle in terms of background Schwarzschild coordinate r . The second and the third columns show the leading and the sub-leading regularization parameters that we get by a numerical matching. The fourth and the fifth columns show the fractional difference between the numerical and the analytic values.

with A^\pm and B given by [9]

$$A_{\text{analytic}}^\pm = \mp \frac{(1 - 3M/r_0)^{1/2}}{r_0^2}, \quad (51a)$$

$$B_{\text{analytic}} = - \frac{\left(\left(1 - \frac{3M}{r_0}\right) \left(1 - \frac{2M}{r_0}\right) \right)^{1/2}}{r_0^2} \left(F_{1/2} - \frac{1}{2} \frac{1 - 3M/r_0}{1 - 2M/r_0} F_{3/2} \right), \quad (51b)$$

where

$$F_p = \frac{2}{\pi} \int_0^{\pi/2} \left(1 - \frac{M}{r_0 - 2M} \sin^2 \Phi \right)^{-p} d\Phi. \quad (52)$$

Table III shows the agreement between the regularization coefficients that we get in a radiation gauge and the ones in the Lorenz gauge.

The renormalized self-force is given by $f^r = \mathbf{m}a^r$, with

$$a^{\text{ren } r} = \sum_{\ell=0}^{\infty} (a^{\text{ret } r}[\ell] - A^\pm L - B). \quad (53)$$

r_0/M	F^r/μ^2
6	0.031741815
7	0.024314669
8	0.019541501
9	0.016137918
10	0.013580536
11	0.011595880
12	0.010019806
13	0.0087455255
14	0.0076999148
15	0.0068310918
16	0.0061012423
18	0.0049526422
20	0.0040997900
25	0.0027292140
30	0.0019459393
35	0.0014569286
40	0.0011313990
45	0.00090387369
50	0.00073864055
60	0.00051979901
70	0.00038553381
80	0.00029728330
90	0.00023619526

TABLE IV: The radial self-force for a particle in circular orbit around a Schwarzschild black hole. The first column lists the Schwarzschild radial coordinate of the orbit; the second gives the radial component of the self-force per unit mass square.

We can add parts of the perturbation corresponding to a change in mass, and angular momentum in any convenient gauge. They, together with an even-parity $l = 1$ gauge transformation outside r_0 that accounts for a change in the center of mass, have been computed in a Lorenz gauge by Poisson and Detweiler, and we use their results. Note that the singular part of the self-force is given by the coefficients in the large- L expansion of the metric and is therefore independent of the choice of gauge for $\ell = 0$ and $\ell = 1$. Our results for the self-force, expressed as the self-acceleration $a_r = f_r/m$, are tabulated in Table IV.

IV. GAUGE-INVARIANT QUANTITIES

The perturbed metric of a particle in circular orbit in a Schwarzschild spacetime is helically symmetric: The helical Killing vector $k^\alpha = t^\alpha + \Omega\phi^\alpha$ of the background spacetime Lie derives the particle's trajectory and is a Killing vector of the linearized metric $h_{\alpha\beta}^{\text{ret}}$ in a Lorenz, Regge-Wheeler, or radiation gauge. As Detweiler noted [3, 10], the quantity $H := h_{\alpha\beta}u^\alpha u^\beta/2$ is invariant under gauge transformations generated by a gauge vector ξ^α that shares this symmetry,

$$\mathcal{L}_{\mathbf{k}}\xi^\alpha = 0. \quad (54)$$

A quick covariant derivation follows from the background geodesic equation in the form $u^\beta\nabla_\beta u^\alpha = 0$ and the relation $u^\alpha = u^t k^\alpha$, where u^t is the scalar $u^\alpha\nabla_\alpha t$. The change in H under a gauge transformation is given by $\delta_\xi H = u^\alpha u^\beta \nabla_\alpha \xi_\beta$. Then

$$u^\alpha u^\beta \nabla_\alpha \xi_\beta = -u^t u^\beta \xi_\alpha \nabla_\beta k^\alpha = -u^\beta \xi_\alpha \nabla_\beta u^\alpha = 0, \quad (55)$$

where Eq. (54) is used in the first equality and the geodesic equation, together with $k^\alpha\nabla_\alpha(u^t) = 0$, is used to obtain the second.

In this section we describe the computation of the renormalized invariant H and, in effect, compare its values at different orbital radii to the values computed in two different gauges by Barack and Sago and by Detweiler. As we show in Appendix A of I, the transformation from a Lorenz gauge to the partial radiation gauge we use is generated by a helically symmetric gauge vector; the value of H^{ren} in our radiation gauge must therefore coincide up to numerical error with its value for a Lorenz gauge. The $\ell = 0$ part of the gauge transformation from a Lorenz gauge to the Regge-Wheeler gauge, however, is not helically symmetric, and we must take account of the gauge change in H to compare our value to the Regge-Wheeler value.

As we discuss below, instead of H itself, Sago et al. tabulate a related gauge-invariant quantity that they term ΔU , which is given in terms of H and the background geometry. To facilitate the comparison to their work, we use ΔU as the quantity to tabulate.

To compute H^{ren} at the position of the particle, we use the harmonic decomposition of the metric to write

$$H^{\text{ret}} = \sum_{\ell m} H_{\ell m} Y_{\ell m}(\pi/2, 0). \quad (56)$$

We then match the sequence of values,

$$H_\ell^{\text{ret}} = \sum_m H_{\ell m} Y_{\ell m}(\pi/2, 0), \quad (57)$$

to a power series in ℓ of the form

$$E_0 + \frac{E_2}{(\ell - 1/2)(\ell + 3/2)} + \frac{E_4}{(\ell - 3/2)(\ell - 1/2)(\ell + 3/2)(\ell + 5/2)} + \dots \quad (58)$$

Because the series is obtained from H^{ret} , the renormalization coefficients E_k are again invariant under helically symmetric gauge transformations, and we compare in Table V the leading term E_0 to an analytic form derived by Detweiler,

$$E_{0 \text{ analytic}} = \sqrt{\frac{r - 3M}{r^2(r - 2M)}} {}_2F_1\left(\frac{1}{2}, \frac{1}{2}, 1, \frac{M}{r - 2M}\right). \quad (59)$$

When H^{ret} is decomposed as a mode sum, the information of the singular part is stored in higher ℓ s. We obtain the leading term by matching H_ℓ^{ret} to a power series in ℓ from $\ell \simeq 15$ to 85. The method of matching is explained in Sec. V below.

Table V shows the fractional error with which the leading coefficient E_0 differs from its analytic form for a set of different radii.

In comparing quantities that we compute in a radiation gauge to those computed by Barack and Sago in a Lorenz gauge and by Detweiler in a Regge-Wheeler gauge, we follow the terminology in Sago et al. [4], using the abbreviations *BS* and *SD* to refer to quantities computed in the two different gauges. We have already mentioned that the comparison

r_0/M	$ \Delta E_0/E_0 $
6	3.8×10^{-14}
7	1.6×10^{-14}
8	9.0×10^{-16}
9	9.0×10^{-15}
10	1.1×10^{-15}
11	5.6×10^{-15}
12	6.0×10^{-16}
13	2.4×10^{-15}
14	1.1×10^{-15}
15	3.4×10^{-15}
16	2.7×10^{-15}
18	4.0×10^{-16}
20	2.0×10^{-15}
25	2.3×10^{-15}
30	1.4×10^{-15}
40	7.0×10^{-16}
50	1.2×10^{-15}
60	1.7×10^{-15}
70	$< 10^{-16}$
80	5.0×10^{-16}

TABLE V: The first column shows the radius of the orbiting particle in terms of the background Schwarzschild coordinate. The second column shows the fractional error in E_0 , $\Delta E_0/E_0 = |E_{0 \text{ numerical}} - E_{0 \text{ analytic}}|/E_{0 \text{ analytic}}$.

requires a correction arising from the lack of helical symmetry in the $l = 0$ gauge vector, but there is an additional difference between the BS and SD computations: BS parametrize the perturbed trajectory by proper time τ with respect to the background metric, while SD uses proper time $\hat{\tau}$ with respect to the renormalized perturbed metric.¹ From the relations

$$\hat{u}^\alpha = u^\alpha \frac{d\tau}{d\hat{\tau}}, \quad (g_{\alpha\beta} + h_{\alpha\beta}^{\text{ren}})\hat{u}^\alpha \hat{u}^\beta = 1 = g_{\alpha\beta} u^\alpha u^\beta, \quad (60)$$

we have, to linear order in the perturbation,

$$\frac{d\tau}{d\hat{\tau}} = 1 - \frac{1}{2} h_{\alpha\beta}^{\text{ren}} u^\alpha u^\beta. \quad (61)$$

Because we, like BS, use proper time with respect to the background metric, we have chosen a Lorenz gauge for the $l = 0$ and $l = 1$ parts of the perturbation so that our u^t will coincide with that of BS. In comparing to SD, we then need both corrections – from the $l = 0$ gauge transformation and from the reparametrization of the trajectory, as given in Sago et al. [4]. The $\ell = 0$ gauge transformation has gauge vector $\xi^\alpha = \alpha t^\alpha$, with

$$\alpha = \mathbf{m}/\sqrt{r_0(r_0 - 3M)}. \quad (62)$$

The relation between u^t in our modified radiation gauge and in a Lorenz gauge (normalized by proper time with respect to the background metric) and \hat{u}^t in a Regge-Wheeler gauge (normalized by proper time with respect to the perturbed metric) is then

$$\hat{u}^t = u^t(1 + \alpha - H^{\text{ren}}) + O(\mathbf{m}^2), \quad (63)$$

¹ To maintain a notation consistent with the EMRI literature and with our previous papers, we denote by u^α the four-velocity normalized with respect to the background metric, with τ the corresponding background proper time. Sago et al. use \tilde{u}^α and $\tilde{\tau}$ for these quantities and their quantities with no tilde correspond to proper time with respect to the perturbed metric.

where H^{ren} , given by

$$H^{\text{ren}} = \frac{1}{2} h_{\alpha\beta}^{\text{ren}} u^\alpha u^\beta, \quad (64)$$

is computed in our modified radiation gauge. Because H^{ret} is invariant under helically symmetric gauge transformations, H^{ren} is similarly invariant.

Following Sago et al., we write $U = \widehat{u}^t$ and construct from it another quantity that is invariant under helically symmetric gauge transformations by expressing the unperturbed U as a function of Ω : With

$$\mathcal{U}_0(\Omega) := (1 - 3M/R)^{-1/2}, \quad R := \left(\frac{M}{\Omega^2}\right)^{1/3}, \quad (65)$$

the unperturbed values U_0 and Ω_0 satisfy

$$U_0 = \mathcal{U}_0(\Omega_0). \quad (66)$$

Then ΔU is defined as the difference

$$\Delta U := U - \mathcal{U}_0(\Omega) = U - (1 - 3M/R)^{-1/2}, \quad (67)$$

where the angular velocity that appears in $\mathcal{U}_0(\Omega)$ is the angular velocity of the perturbed trajectory. One can express ΔU in terms of H using the changes $\delta\Omega$ and δU in Ω and U due to a self-force whose only component is radial, $f_r = \mathbf{m}a_r$, namely

$$\delta\Omega = \Omega - \Omega_0 = -\Omega_0 \frac{r_0^2(1 - 3M/r_0)}{2M} a_r + O(\mathbf{m}^2), \quad (68)$$

$$\delta U = U - U_0 = U_0 \left(-H^{\text{ren}} - \frac{r_0}{2} a_r\right) + O(\mathbf{m}^2), \quad (69)$$

to obtain

$$\Delta U = -(1 - 3M/r_0)^{-1/2} H^{\text{ren}}. \quad (70)$$

Note that ΔU is gauge-invariant in the standard sense that it has the same value when $h_{\alpha\beta}$ is replaced by $h_{\alpha\beta} + \mathcal{L}_\xi g_{\alpha\beta}$ (in this case, when ξ^α is helically symmetric). Detweiler and Sago et al. [3, 4, 10] also use the term ‘‘gauge-invariant’’ to refer to the finite quantities U and Ω . Their terminology is motivated by the fact that Ω and U are physically meaningful: In particular, Ω can be measured by an observer at infinity from the periodicity of received signals sent at equally spaced proper times from the orbiting particle.

One must be careful, however, because $\delta\Omega$ and δU are not gauge invariant. With the standard definition of the change of a scalar on spacetime under a gauge transformation generated by a gauge vector ξ^α , they change by

$$\delta\Omega \rightarrow \delta\Omega + \mathcal{L}_\xi \Omega, \quad \delta U \rightarrow \delta U + \mathcal{L}_\xi U. \quad (71)$$

Note, in particular, that Sago et al. use symbols $\delta_\xi \Omega$ and $\delta_\xi U$ whose meaning is different from the change in Ω and U under a gauge transformation, while their symbol $\delta_\xi h_{\alpha\beta}$ *does* have the meaning $\mathcal{L}_\xi g_{\alpha\beta}$. We discuss the terminology and the reason ΔU is invariant under helically symmetric gauge transformations in the Appendix.

Because we have used the Lorenz gauge for the $\ell = 0$ and $\ell = 1$ parts of the metric perturbation (derived by Detweiler and Poisson), and the gauge transformation from a Lorenz gauge to the Regge-Wheeler gauge of Detweiler is not helically symmetric, we need to make the same gauge adjustment made by BS to our ΔU to compare its the value to that of Detweiler, namely

$$\Delta U^{\text{D}} = (1 - 3M/r_0)^{-1/2} \left(\frac{r_0 - 2M}{r_0 - 3M} \alpha - H^{\text{ren, RG}} \right). \quad (72)$$

In the comparison table, Table VI below, ΔU is given in the Regge-Wheeler gauge used by Detweiler. The table reports results of the computation performed in the three gauges, radiation, Regge-Wheeler, and Lorenz.

r_0/M	ΔU	$\Delta U(\text{from SD})$	$\Delta U(\text{from BS})$
6	-0.29602751	-0.2960275	-0.296040244
7	-0.22084753	-0.2208475	-0.220852781
8	-0.17771974	-0.1777197	-0.177722443
9	-0.14936061	-0.1493606	-0.149362192
10	-0.12912227	-0.1291222	-0.129123253
11	-0.11387465	-0.1138747	-0.113875315
12	-0.10193557	-0.1019355	-0.101936046
13	-0.092313311	-0.09231331	-0.092313661
14	-0.084381953	-0.08438195	-0.084382221
15	-0.077725319	-0.07772532	-0.077725527
16	-0.072055057	-0.07205505	-0.072055223
18	-0.062901899	-0.06290189	-0.062902026
20	-0.055827719	-0.05582771	-0.055827795
25	-0.043599843	-0.04359984	-0.043599881
30	-0.035778314	-0.03577831	-0.035778334
40	-0.026339677	-0.02633967	-0.026339690
50	-0.020844656	-0.02084465	-0.020844661
60	-0.017247593	-0.01724759	-0.017247596
70	-0.014709646	-0.01470964	-0.014709648
80	-0.012822961	-0.01282296	-0.012822962
90	-0.011365316	-0.01136531	-0.011365317

TABLE VI: In this table we compare our values of ΔU with BS and SD. The first column shows the radius of the orbiting particle in terms of background Schwarzschild coordinate. The second, third and fourth column shows the values of ΔU computed in a radiation gauge, Regge-Wheeler gauge (SD) and Lorenz gauge (BS).

V. NUMERICAL MATCHING

As mentioned in Paper I, we find the singular part of the self-force by matching a power series to its numerically computed large- L behavior. Explicitly, we match the sequence of values $a^{\text{ret}}[\ell]$ to successive terms in a series of the form

$$AL + B + \sum_{k=1}^{k_{\text{max}}} \frac{\tilde{E}_{2k}}{P_{2k}(\ell)}, \quad (73)$$

where the polynomial,

$$P_{2k}(\ell) = \prod_{i=1}^k \left(\ell - k - \frac{1}{2} + i \right) \prod_{j=1}^k \left(\ell + k + \frac{3}{2} - j \right), \quad (74)$$

satisfies

$$\sum_{\ell=0}^{\infty} \frac{1}{P_{2k}(\ell)} = 0. \quad (75)$$

When one matches the above series to the numerical series $a^{\text{ret}}[\ell]$ over a range $\ell_{\text{min}} \leq \ell \leq \ell_{\text{max}}$, the accuracy with which A and B are obtained depends on the value of k_{max} chosen – on the number of parameters E_{2k} used in the matching. We choose k_{max} to minimize the difference $(A_{(k_{\text{max}}+1)} - A_{k_{\text{max}}})/A_{k_{\text{max}}}$ as a function of k_{max} . For ℓ_{max} infinite and no numerical error, $A_{(k_{\text{max}}+1)} - A_{k_{\text{max}}}$ would converge to zero as $k_{\text{max}} \rightarrow \infty$. For finite ℓ_{max} only a finite number of parameters can be extracted, and we approximate the value of k_{max} for which A and B are most accurately determined by the value \tilde{k} of k_{max} that minimizes $A_{(k_{\text{max}}+1)} - A_{k_{\text{max}}}$.

We check this approximation by using our knowledge of the analytic form of the leading renormalization parameter

E_0 in the quantity $h_{\alpha\beta}u^\alpha u^\beta = 2H$:

$$2H^{\text{sing}} = E_0 + \sum_{k=1}^{k_{\text{max}}} \frac{E_{2k}}{P_{2k}(\ell)}. \quad (76)$$

In Fig. 1, we compare \tilde{k} to the value of k_{max} that minimizes the error in E_0 . The graph shows for a particular orbital radius that the error in E_0 is a minimum at a value of k_{max} in the interval $\tilde{k} \pm 1$.

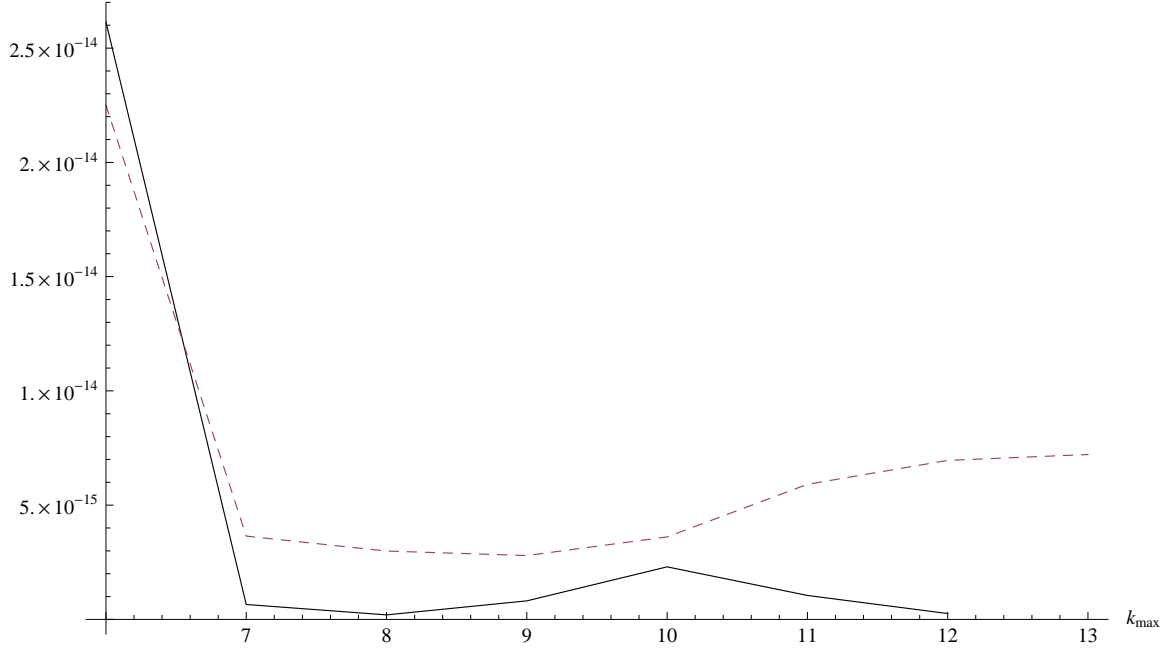


FIG. 1: The solid curve is a plot of $|E_{0(k_{\text{max}}+1)} - E_{0k_{\text{max}}}|/E_{0k_{\text{max}}}$ vs k_{max} . The dashed curve is a plot of $|E_{0\text{analytic}} - E_{0\tilde{k}}|/(E_{0\text{analytic}})$ as a function of k_{max} . Both are for orbital radius $r_0 = 10M$

Table VII shows for a set of orbital radii the minimum value of $|E_{0(k_{\text{max}}+1)} - E_{0k_{\text{max}}}|/E_{0k_{\text{max}}}$, its value at $k_{\text{max}} = \tilde{k}$; that is compared to the value of $|E_{0\text{analytic}} - E_{0k_{\text{max}}}|/E_{0\text{analytic}}$, again at $k_{\text{max}} = \tilde{k}$. One can infer from the table that, by minimizing $A_{(k_{\text{max}}+1)} - A_{k_{\text{max}}}$, one obtains values of the renormalization parameters to a fractional precision of 10^{-13} or better. Similar accuracy was reported in Paper I for the leading renormalization parameter in the axisymmetric part of ψ_0 .

r_0/M	minimum of $\frac{E_{0(k_{\max}+1)} - E_{0k_{\max}}}{E_{0k_{\max}}}$	$\frac{E_{0analytic} - E_{0\tilde{k}}}{E_{0analytic}}$
6	1.4×10^{-14}	1.4×10^{-14}
7	1.5×10^{-15}	1.1×10^{-14}
8	1.7×10^{-15}	1.3×10^{-15}
9	3.0×10^{-16}	8.4×10^{-15}
10	2.0×10^{-16}	3.0×10^{-15}
11	8.0×10^{-16}	3.8×10^{-15}
12	$< 10^{-16}$	2.7×10^{-15}
13	3.0×10^{-16}	5.0×10^{-16}
14	2.0×10^{-16}	5.1×10^{-15}
15	2.0×10^{-16}	9.0×10^{-16}
16	$< 10^{-16}$	1.7×10^{-15}
18	2.0×10^{-16}	2.0×10^{-16}
20	$< 10^{-16}$	2.0×10^{-15}
25	$< 10^{-16}$	2.5×10^{-15}
30	4.0×10^{-16}	6.0×10^{-16}
40	3.0×10^{-16}	5.0×10^{-16}
50	2.0×10^{-16}	1.1×10^{-15}
60	6.0×10^{-16}	1.4×10^{-15}
70	$< 10^{-16}$	3.0×10^{-16}
80	2.0×10^{-16}	$< 10^{-16}$

TABLE VII: The first column shows the radius of the orbiting particle in terms of background Schwarzschild coordinate r . The second column shows the minimum of $|E_{0(k_{\max}+1)} - E_{0k_{\max}}|/E_{0k_{\max}}$ as a function of k_{\max} . Let that k_{\max} be denoted as \tilde{k} . The third column shows the quantity $|E_{0analytic} - E_{0\tilde{k}}|/(E_{0analytic})$. $\ell_{\min} = 15$.

The accuracy with which the values of E_k are obtained also depends on the values of ℓ_{\min} and ℓ_{\max} . For fixed ℓ_{\max} , there is an optimal value of ℓ_{\min} that minimizes the error in the regularization parameters. For higher ℓ_{\min} , contributions of the higher-order E_{2k} are too small to extract; for small ℓ_{\min} the $H^{\text{ret}}[\ell]$ (or $a^{\text{ret}} r[\ell]$) will depart from its large- L behavior. Tables VIII and IX show the behavior of the regularization parameters for different choice of ℓ_{\min} (for a fixed $\ell_{\max} = 84$) at two different radii. Increasing ℓ_{\max} , of course, increases the accuracy of the computation.

ℓ_{\min}	0	-2	-4	-6	-8	$\frac{E_{0analytical} - E_{0\tilde{k}}}{E_{0analytical}}$	\tilde{k}
5	5×10^{-13}	1×10^{-9}	9×10^{-7}	4×10^{-4}	1×10^{-3}	6×10^{-13}	10
10	4×10^{-17}	8×10^{-13}	2×10^{-9}	4×10^{-6}	5×10^{-5}	7×10^{-16}	11
15	2×10^{-16}	7×10^{-12}	4×10^{-8}	1×10^{-4}	4×10^{-3}	8×10^{-16}	10
20	2×10^{-15}	9×10^{-11}	6×10^{-7}	3×10^{-3}	1×10^{-1}	2×10^{-15}	7
25	7×10^{-16}	4×10^{-11}	3×10^{-7}	1×10^{-3}	6×10^{-2}	2×10^{-15}	6

TABLE VIII: This table shows the first five fractional differences between successive regularization parameters in the singular part of $2H$ for five different values of ℓ_{\min} , with $k_{\max} = \tilde{k}$. The second, third, fourth, fifth and the sixth columns list the fractional differences $(|E_{n,\tilde{k}+1} - E_{n,\tilde{k}}|/E_{n,\tilde{k}})$ for $n = 0, -2, -4, -6, -8$, respectively. The seventh column gives the fractional difference between $E_{0analytical}$ and $E_{0\tilde{k}}$. The last column gives \tilde{k} . All values are for orbital radius $r_0 = 15M$.

The number of renormalization parameters needed to attain machine accuracy is small, because the errors in the

ℓ_{\min}	0	-2	-4	-6	-8	$\frac{E_{0\text{analytical}} - E_{0\tilde{k}}}{E_{0\text{analytical}}}$	\tilde{k}
5	2×10^{-13}	9×10^{-9}	4×10^{-6}	7×10^{-3}	2×10^{-3}	7×10^{-12}	10
10	6×10^{-18}	9×10^{-14}	1×10^{-10}	1×10^{-6}	2×10^{-6}	3×10^{-15}	11
15	2×10^{-16}	6×10^{-12}	2×10^{-8}	4×10^{-4}	2×10^{-3}	3×10^{-15}	8
20	2×10^{-16}	7×10^{-12}	4×10^{-8}	2×10^{-3}	2×10^{-2}	3×10^{-16}	9
25	1×10^{-15}	5×10^{-11}	3×10^{-7}	9×10^{-3}	7×10^{-2}	2×10^{-15}	7

TABLE IX: Entries are as in Table VIII, with $r_0=10M$.

mode sums are of order

$$\sum_{\ell=85}^{\infty} \frac{1}{P_{10}(\ell)} \sim \sum_{\ell=84}^{\infty} \frac{1}{(\ell + 1/2)^{10}} \sim 10^{-19}, \quad (77)$$

$$\sum_{\ell=85}^{\infty} \frac{1}{P_8(\ell)} \sim \sum_{\ell=84}^{\infty} \frac{1}{(\ell + 1/2)^8} \sim 10^{-15}$$

and the |reg parameter| < 1. We work to a fractional error of order 10^{13} , terminating the sum over k in Eq. (78) at $k_{\max} = 3$.

Figure 2 shows the result of subtracting successive terms in the numerically-determined large- L expansion of the self-force, using $a^{\text{ret } r} = f^{\text{ret } r}/m$, for a particle at $r_0 = 10M$.

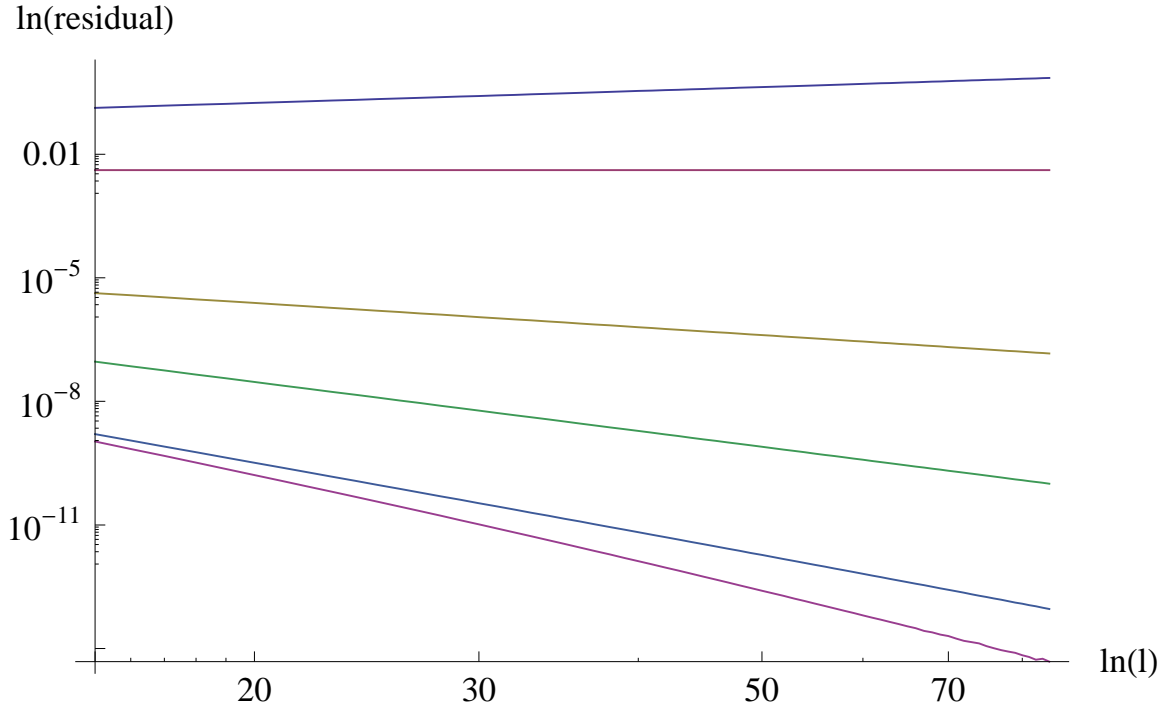


FIG. 2: This figure shows a plot of $\log a_{\ell}^{\text{ret } r}$ (and subsequent subtractions of the singular terms) vs $\log \ell$. The topmost curve is $a_{\ell}^{\text{ret } r} \sim \ell$. The second curve (from the top) is $(a_{\ell}^{\text{ret } r} - A(\ell + 1/2)) \sim \ell^0$. The third curve shows $(a_{\ell}^{\text{ret } r} - A(\ell + 1/2) - B) \sim \ell^{-2}$. The fourth, fifth and sixth curves show the subsequent cumulative subtractions of $E_2/P_2(\ell)$, $E_4/P_4(\ell)$ and $E_6/P_6(\ell)$ from the third.

Each successive subtraction should reduce the slope of the $\log \ell$ vs $\log f^{\text{ret } r}[\ell]$ curve by an integer, and the computed graphs shows the expected behavior for the first four renormalization coefficients.

The accuracy with which the higher-order renormalization coefficients can be computed can be used to estimate the accuracy with which H^{ren} and $f^{\text{ren } r}$ are computed. In addition, once the E_{2k} have been found, the terms in the mode sum can be grouped as a rapidly convergent numerical sum and an analytically known sum. We have

$$\begin{aligned} f^{\text{ren},r} &= \sum_{\ell=0}^{\infty} [f_{\ell}^{\text{ret } r} - A(\ell + 1/2) - B] \\ &= \left(\sum_{\ell=0}^{\ell_{\text{max}}} + \sum_{\ell_{\text{max}+1}}^{\infty} \right) \left[f_{\ell}^{\text{ret } r} - A(\ell + 1/2) - B - \frac{\tilde{E}_2}{Q_2(\ell)} - \dots - \frac{\tilde{E}_{2k_{\text{max}}}}{Q_{2k_{\text{max}}}(\ell)} \right] + \sum_{\ell=0}^{\infty} \left[\frac{\tilde{E}_2}{Q_2(\ell)} + \dots + \frac{\tilde{E}_{2k_{\text{max}}}}{Q_{2k_{\text{max}}}(\ell)} \right] \\ &= \sum_{\ell=0}^{\ell_{\text{max}}} \left[f_{\ell}^{\text{ret } r} - A(\ell + 1/2) - B - \frac{\tilde{E}_2}{Q_2(\ell)} - \dots - \frac{\tilde{E}_{2k_{\text{max}}}}{Q_{2k_{\text{max}}}(\ell)} \right] + \sum_{\ell=0}^{\infty} \left[\frac{\tilde{E}_2}{Q_2(\ell)} + \dots + \frac{\tilde{E}_{2k_{\text{max}}}}{Q_{2k_{\text{max}}}(\ell)} \right] + O\left(\frac{1}{\ell_{\text{max}}^{2k_{\text{max}}+1}}\right), \end{aligned} \quad (78)$$

where the terms $Q_{2k}(\ell)$ represent any polynomials in ℓ whose first term is ℓ^{2k} . The polynomials can be chosen to allow the second sum on the right side of Eq. (78) to be computed analytically. When the polynomials P_{2k} can be used, as in our calculation, the second sum vanishes.

VI. DISCUSSION

The work here gives a first example of the successful use of a (modified) radiation gauge to compute the self-force on a particle in circular orbit. In comparing the renormalized perturbed metric component $h_{\alpha\beta}u^{\alpha}u^{\beta}$, we obtain agreement to high numerical accuracy with previous calculations in other gauges. The work shows that the singular field can be identified with the singular field in a Lorenz gauge. We verify the coincidence numerically to high precision. It follows analytically from (1) the expression derived in the companion paper [1] for the gauge vector ξ^{α} that relates a Lorenz and radiation gauge and (2) the fact that the gauge transformation of the self-force for a particle in circular orbit involves no derivatives of the gauge vector.

In extending the method to circular orbits in Kerr and then to more general orbits, additional subtleties arise. Although spheroidal harmonics decouple in the Teukolsky equation for ψ_0 and ψ_4 , the lack of spherical symmetry means that angular harmonics with different values of ℓ no longer decouple in the perturbed metric or in the expression for the self-force. This significantly changes the way one computes the contribution to the perturbed metric associated with the change in the center of mass – a perturbation that is purely $\ell = 1$ for a Schwarzschild background. A second complication for non-circular orbits, arises from the existence of a region between periastron and apastron, a region where the time and angular harmonics of ψ_0 have a nonzero source. Ways to handle each of these complications will be discussed in a subsequent paper.

Acknowledgments

We thank Norichika Sago for corrections and helpful comments and Eirini Messaritaki for a number of discussions early in the course of the work on this paper and Paper I. This work was supported in part by NSF Grants PHY 0503366 and PHY 1001515. D.H-K's work was supported by the Alexander von Humboldt Foundation's Sofja Kovalevskaja Programme funded by the German Federal Ministry of Education and Research and by WCU (World Class University) program of NRF/MEST (R32-2009-000-10130-0).

Appendix A: Gauge invariants

As we mentioned in Sec. IV, the symbols $\delta_{\xi}\Omega$ and $\delta_{\xi}U$ used in Refs. [3, 4, 10] in describing U and Ω as gauge-invariant are not the standard definitions of the change in a scalar function under a gauge transformation. The difference in definitions arises because the four-velocity of a single particle does not conform to the framework used to describe perturbations of a set of physical fields on spacetime. The change in the trajectory of a single particle involves a four-velocity that is defined only on a single trajectory, and the trajectory is different for the perturbed and unperturbed spacetimes.

Note that Detweiler and Sago et al. are careful to distinguish a lack of gauge invariance of $\delta\Omega := \Omega - \Omega_0$ and $\delta U := U - U_0$ from the invariance of Ω and U . The number Ω can be measured, for example, by an observer at

infinity from waves received from the orbiting particle: It is in this sense gauge-invariant. However, when Ω is regarded as a function of trajectories or as a function on a Schwarzschild spacetime that assigns to each point of spacetime the frequency of a circular orbit through that point, it becomes gauge-dependent. In particular, in the active description of a gauge transformation, an infinitesimal diffeo changes the metric at a point of spacetime by $\mathcal{L}_\xi g_{\alpha\beta}$, and the frequency of a geodesic through that point then changes by $\mathcal{L}_\xi \Omega$. (In the passive description of a gauge transformation, with Ω regarded as a function of the coordinates, an infinitesimal coordinate transformation correspondingly changes the functional dependence of Ω on the coordinates.)

We give here a brief review of general relativistic perturbation theory and gauge transformations. We describe linearized perturbation in terms of a family of fields, with gauge transformations described in the active sense of diffeos (diffeomorphisms). We begin with a family of metrics $g_{\alpha\beta}(\lambda)$, defining $\delta g_{\alpha\beta}$ as the change in the metric to first order in λ as the quantity

$$\delta g_{\alpha\beta} = \left. \frac{d}{d\lambda} g_{\alpha\beta}(\lambda) \right|_{\lambda=0}. \quad (\text{A1})$$

When no other fields are present, the metric $g_{\alpha\beta}$ is physically equivalent to the diffeomorphically related metric $\psi^* g_{\alpha\beta}$, where ψ is a diffeo (a diffeomorphism) and ψ^* is the pullback, whose components are given by

$$\psi^* g_{\mu\nu}(P) = \frac{\partial \psi^\sigma}{\partial x^\mu} \frac{\partial \psi^\tau}{\partial x^\nu} g_{\sigma\tau}[\psi(P)]. \quad (\text{A2})$$

A gauge transformation is defined by considering a smooth family of diffeos ψ_λ , with ψ_0 the identity. We denote by ξ^α the vector field tangent at each point P to the orbit $\lambda \mapsto \psi_\lambda(P)$ of P . That is, to linear order in λ , a point with coordinates x^μ is mapped to a point with coordinates $\psi^\mu(P) = x^\mu + \lambda \xi^\mu(P)$. The family of metrics $g_{\alpha\beta}(\lambda)$ is then physically equivalent to the family $\psi_\lambda^* g_{\alpha\beta}(\lambda)$, and the metric perturbation $\delta g_{\alpha\beta}$ is physically equivalent to the gauge-related metric perturbation

$$\delta g_{\alpha\beta} + \delta_\xi g_{\alpha\beta} := \left. \frac{d}{d\lambda} \psi_\lambda^* g_{\alpha\beta}(\lambda) \right|_{\lambda=0} = \left. \frac{d}{d\lambda} g_{\alpha\beta}(\lambda) \right|_{\lambda=0} + \left. \frac{d}{d\lambda} \psi_\lambda^* g_{\alpha\beta}(0) \right|_{\lambda=0} = \delta g_{\alpha\beta} + \mathcal{L}_\xi g_{\alpha\beta}. \quad (\text{A3})$$

When other physical fields $[T_1, \dots, T_N]$ are present, the families of fields $[g_{\alpha\beta}(\lambda), T_1(\lambda), \dots, T_N(\lambda)]$ and $[\psi_\lambda^* g_{\alpha\beta}, \psi_\lambda^* T_1, \dots, \psi_\lambda^* T_N]$ describe the same physical system. The corresponding physical equivalence of the perturbed fields, linearized about $\lambda = 0$, is the equivalence of δT and $\delta T + \mathcal{L}_\xi T$, for each physical field T , where

$$\delta T = \left. \frac{d}{d\lambda} T(\lambda) \right|_{\lambda=0}, \quad \delta \psi_\lambda^* T = \left. \frac{d}{d\lambda} [\psi_\lambda^* T(\lambda)] \right|_{\lambda=0} = \delta T + \delta_\xi T, \quad \text{and} \quad \delta_\xi T = \mathcal{L}_\xi T. \quad (\text{A4})$$

In particular, if T is a scalar, $\psi_\lambda^* T = T \circ \psi_\lambda$, implying

$$T(P) = \psi_\lambda^* T[\psi_\lambda^{-1}(P)]. \quad (\text{A5})$$

A scalar f constructed locally from a set of tensor fields T_1, \dots, T_k , with

$$f = F(T_1, \dots, T_k), \quad \text{with} \quad f(P) = F[T_1(P), \dots, T_k(P)], \quad (\text{A6})$$

satisfies

$$\psi f = F(\psi T_1, \dots, \psi T_k), \quad (\text{A7})$$

implying, for any vector field ξ^α ,

$$\mathcal{L}_\xi f = \left. \frac{d}{d\lambda} F(T_1 + \lambda \mathcal{L}_\xi T_1, \dots, T_k + \lambda \mathcal{L}_\xi T_k) \right|_{\lambda=0}. \quad (\text{A8})$$

One also uses a set of reference fields – basis vectors or coordinates, for example – that are independent of λ and are not changed by the diffeo that maps the set of physical fields to the physically equivalent set. For example, with t^α the vector ∂_t , the gauge transformation $\delta_\xi g_{tt}$ of a component $g_{\alpha\beta} t^\alpha t^\beta$ is

$$\delta_\xi g_{tt} = \mathcal{L}_\xi g_{tt} = (\mathcal{L}_\xi g_{\alpha\beta}) t^\alpha t^\beta \neq \mathcal{L}_\xi (g_{\alpha\beta} t^\alpha t^\beta). \quad (\text{A9})$$

We now turn to the problem at hand, the behavior of U and Ω under gauge transformations. These are defined in terms of the four-velocity u^α . To define them and u^α as fields, to write a change δu^α as a vector at a point using

the definition (A4), and to define the Lie derivative $\mathcal{L}_\xi u^\alpha$, one must introduce a set of nearby orbits. In the problem considered here, one can define an unperturbed vector field u^α by taking $u^\alpha(P)$ to be the four-velocity of the circular orbit through P . The perturbed vector field at P is then the four-velocity of the perturbed circular orbit through P . The scalar U of Sec. IV is constructed locally from $g_{\alpha\beta}, \Omega, t^\alpha$, and ϕ^α :

$$U = \mathcal{U}[g_{\alpha\beta}(t^\alpha + \Omega\phi^\alpha)(t^\beta + \Omega\phi^\beta)]^{-1/2} =: \mathcal{U}(g_{\alpha\beta}, \Omega, t^\alpha, \phi^\alpha). \quad (\text{A10})$$

Here t^α and ϕ^α are reference fields, defined as the vectors ∂_t and ∂_ϕ tangent to the coordinate lines, so that they have the same values for the perturbed and unperturbed metric. (Note that they are not Killing fields of the perturbed metric, and cannot be defined in this way.) If ξ^α is helically symmetric with respect to $k^\alpha = t^\alpha + \Omega(P)\phi^\alpha$, for a given fixed P , then

$$\delta_\xi U(P) = \left. \frac{d}{d\lambda} \mathcal{U}(g_{\alpha\beta} + \lambda \mathcal{L}_\xi g_{\alpha\beta}, \Omega + \lambda \mathcal{L}_\xi \Omega, t^\alpha, \phi^\alpha) \right|_{\lambda=0} = \mathcal{L}_\xi U(P). \quad (\text{A11})$$

Similarly,

$$\delta_\xi \Omega(P) = \mathcal{L}_\xi \Omega(P). \quad (\text{A12})$$

Finally, defining \mathcal{U}_0 as in Eq. (66), we have

$$\delta_\xi [U - \mathcal{U}_0(\Omega)] = [\mathcal{L}_\xi U - \mathcal{L}_\xi \mathcal{U}_0]_{\lambda=0} = \mathcal{L}_\xi U_0 - \mathcal{L}_\xi U_0 = 0. \quad (\text{A13})$$

That, is, $U - \mathcal{U}_0(\Omega)$ is gauge invariant in the usual sense, for helically symmetric gauge vectors.

If we denote by $\widehat{\delta}_\xi U$ and $\widehat{\delta}_\xi \Omega$ the changes in U and Ω introduced by Sago et al., Eqs. (A11) and (A12) are equivalent to writing

$$\widehat{\delta}_\xi U = 0, \quad \widehat{\delta}_\xi \Omega = 0. \quad (\text{A14})$$

Although any scalar constructed locally from physical fields alone has this behavior, Eqs. (A11) and (A12) (or, equivalently, (A14)) are not trivial relations, because they involve reference fields that do not change under gauge transformations.

The difference between δ_ξ and $\widehat{\delta}_\xi$ is the change associated with a second kind of gauge freedom, mentioned in Appendix A.2 of Paper I, namely an infinitesimal change (by a displacement ξ^α) in the background geodesic to which one compares a geodesic in the perturbed spacetime.

-
- [1] T. S. Keidl, A. G. Shah, D. H. Kim, J. L. Friedman, and L. R. Price (2010), arXiv:1004.2276v2.
 - [2] L. Barack and N. Sago, Phys. Rev. D **75**, 064021 (2007), arXiv:gr-qc/0701069.
 - [3] S. Detweiler, Phys. Rev. D **77**, 124026 (2008), 0804.3529.
 - [4] N. Sago, L. Barack, and S. Detweiler, Phys. Rev. D **78**, 124024 (2008), 0810.2530.
 - [5] Y. Mino, M. Sasaki, and T. Tanaka, Phys. Rev. D **55**, 3457 (1997), arXiv:gr-qc/9606018.
 - [6] T. C. Quinn and R. M. Wald, Phys. Rev. D **56**, 3381 (1997), arXiv:gr-qc/9610053.
 - [7] S. E. Gralla, In preparation: See Talk at 2010 Capra Meeting, <http://pirsa.org/10060049> (2010).
 - [8] S. E. Gralla and R. M. Wald, Classical and Quantum Gravity **25**, 205009 (2008), 0806.3293.
 - [9] S. Detweiler, E. Messaritaki, and B. F. Whiting, Phys. Rev. D **67**, 104016 (2003), arXiv:gr-qc/0205079.
 - [10] S. Detweiler, Classical and Quantum Gravity **22**, S681 (2005), arXiv:gr-qc/0501004.